

Kinetics of the $R + HBr \rightleftharpoons RH + Br$ ($R = CH_2Br$, $CHBrCl$ or CCl_3) equilibrium. Thermochemistry of the CH_2Br and $CHBrCl$ radicals

Jorma A. Seetula

Laboratory of Physical Chemistry, P.O. Box 55, (A. I. Virtasen aukio 1), FIN-00014, University of Helsinki, Helsinki, Finland. E-mail: seetula@csc.fi

Received 1st November 2002, Accepted 3rd January 2003

First published as an Advance Article on the web 24th January 2003

The kinetics of the reaction of the CH_2Br , $CHBrCl$ or CCl_3 radicals, R , with HBr have been investigated separately in a heatable tubular reactor coupled to a photoionization mass spectrometer. The CH_2Br (or $CHBrCl$ or CCl_3) radical was produced homogeneously in the reactor by a pulsed 248 nm exciplex laser photolysis of CH_2Br_2 (or $CHBr_2Cl$ or $CBrCl_3$). The decay of R was monitored as a function of HBr concentration under pseudo-first-order conditions to determine the rate constants as a function of temperature. The reactions were studied separately over a wide ranges of temperatures and in these temperature ranges the rate constants determined were fitted to an Arrhenius expression (error limits stated are 1σ + Student's t values, units in cm^3 molecule $^{-1}$ s $^{-1}$): $k(CH_2Br + HBr) = (7.5 \pm 0.9) \times 10^{-13} \exp[-(2.53 \pm 0.13) \text{ kJ mol}^{-1}/RT]$, $k(CHBrCl + HBr) = (4.9 \pm 1.1) \times 10^{-13} \exp[-(8.2 \pm 0.3) \text{ kJ mol}^{-1}/RT]$ and $k(CCl_3 + HBr) < (6 \pm 1) \times 10^{-15}$ at 787 K. The kinetics of the reverse reactions, $Br + R'H \rightarrow HBr + R'$ ($R' = CH_2Br$ or $CHBrCl$), were taken from the literature and also calculated by *ab initio* methods at the MP2(fc)/6-31G(d,p)//MP2(fc)/6-31G(d,p) level of theory in conjunction with the thermodynamic transition state theory to calculate the entropy and the enthalpy of formation values of the radicals studied. The thermodynamic values were obtained at 298 K using a second-law method. The results for entropy values are as follows (units in $J K^{-1} \text{ mol}^{-1}$): 263 ± 7 (CH_2Br) and 294 ± 6 ($CHBrCl$). The results for enthalpy of formation values at 298 K are (in kJ mol^{-1}): 171.1 ± 2.7 (CH_2Br) and 143 ± 6 ($CHBrCl$). The C–H bond strength of analogous halomethanes are (in kJ mol^{-1}): 427.2 ± 2.4 (CH_3Br) and 406.0 ± 2.4 (CH_2BrCl). Thermodynamic properties of the CH_2Br radical were calculated by statistical thermodynamic methods over the temperature range 100–1500 K.

Introduction

The natural source of bromomethane has been found to be a marine phytoplankton.¹ Bromomethane is considered to be the most abundant atmospheric source of bromine atoms, which recently have been considered to take a part in the catalytic destruction of ozone in the Earth's atmosphere. Bromomethane is a very toxic compound and it is generally prepared from a reaction of hydrogen bromide with methanol. It is used for methylation in organic synthesis and as a fumigant. The concentration of bromomethane in atmosphere is largely limited by its reactions with atoms and OH radical where CH_2Br radical is the product of these reactions. Of these, the reaction with OH has a principal loss process for atmospheric bromomethane. The CH_2Br radical may react further in exothermic reactions with other open shell species at atmospheric conditions to release Br atoms for secondary reactions with ozone. The other product from this reaction is BrO which self-reaction produces molecular bromine and oxygen. A similar set of elementary reactions may be considered to occur for bromochloromethane. It has also considered as an effective fire suppressant. Both bromomethane as well as bromochloromethane have been detected at lower stratosphere among other brominated compounds.²

Another function of the current study is on fundamental understanding of free radical kinetics and reactivity with hydrogen halides. These include both alkyl and halogenated alkyl free radicals. Accurate kinetic information of the both reaction directions provide enthalpy and free energy changes for the overall reaction under study from which the enthalpy of formation of the free radical can be determined. Moreover,

this information establishes the magnitudes of the various C–H bond strengths which are associated with the enthalpy change of the following reaction: radical–H \rightarrow radical + H.

The current study presents a time-resolved experimental kinetic investigation of the CH_2Br , the $CHBrCl$ and the CCl_3 radicals with HBr . The reactions have not previously been studied. Two of the reactions were studied over a wide temperature range and $CCl_3 + HBr$ reaction only at temperature of 787 K. The approach for all three reactions is similar as that used for the study of chlorinated radicals with HBr .³ The current study was carried out to investigate the enthalpy of formation of the CH_2Br and of the $CHBrCl$ radicals using a second-law method. The kinetics of the reverse reaction direction $Br + RH \rightarrow HBr + R$ was taken from the literature and also studied theoretically. Different reaction channels of the $Br + CH_3Br/CH_2BrCl$ reactions were studied by *ab initio* methods. The enthalpy of reactions were later used to calculate C–H bond energies of analogous halogenated methanes. These values were compared with other C–H bond energies of hydrocarbons and halogenated hydrocarbons.

Kinetics and computational

Description of kinetic experiments

The rate constants of the reaction of CH_2Br or $CHBrCl$ with HBr were measured as a function of the temperature range. The experimental apparatus used has been previously described.^{4,5} Pulsed, unfocused 248 nm radiation from a Lambda Physik EMG 201 MSC exciplex laser operated at

Table 1 Measurements of the rate constant of the $R + \text{HBr} \rightarrow \text{RH} + \text{Br}$ ($R = \text{CH}_2\text{Br}$, CHBrCl or CCl_3) reaction

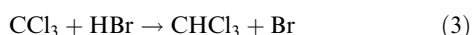
T^a/K	$[\text{He}]/10^{16} \text{ cm}^{-3}$	$[\text{HBr}]/10^{14} \text{ cm}^{-3}$	k_4/s^{-1}	Wall	$k_1^b/10^{-13} \text{ cm}^3 \text{ s}^{-1}$
$\text{CH}_2\text{Br} + \text{HBr} \rightarrow \text{CH}_3\text{Br}$ (k_1)					
299	5.81	2.71–7.51	3.4	HW	2.76 ± 0.15
300	17.7	1.24–9.52	3.6	HW	2.80 ± 0.16
348	5.83	1.62–5.31	3.9	HW	3.06 ± 0.18
348	5.90	1.77–5.20	10	PDMS	3.07 ± 0.22
409	5.85	2.11–9.68	7.7	PDMS	3.46 ± 0.17
510	5.86	0.99–3.97	19	PDMS	4.11 ± 0.26
510	5.86	1.74–4.79	5.5	B_2O_3	4.15 ± 0.14
677	5.89	1.96–3.92	6.9	B_2O_3	5.3 ± 0.6
$k_1 = (7.5 \pm 0.9) \times 10^{-13} \exp[-(2.53 \pm 0.13) \text{ kJ mol}^{-1}/RT] \text{ cm}^3 \text{ molecule}^{-1} \text{ s}^{-1}$					
$\text{CHBrCl} + \text{HBr} \rightarrow \text{Br} + \text{CH}_2\text{BrCl}$ (k_2)					
414	11.9	5.47–22.2	3.2	B_2O_3	0.48 ± 0.02
457	11.9	2.90–15.2	1.9	B_2O_3	0.57 ± 0.02
511	5.85	3.69–11.0	0.0	B_2O_3	0.69 ± 0.03
579	5.88	5.48–10.3	0.7	B_2O_3	0.84 ± 0.03
667	5.90	5.32–12.1	1.5	B_2O_3	1.06 ± 0.03
722	5.91	2.84–9.28	0.0	B_2O_3	1.25 ± 0.03
787	5.92	3.72–8.47	0.1	B_2O_3	1.58 ± 0.08
$k_2 = (4.9 \pm 1.2) \times 10^{-13} \exp[-(8.2 \pm 0.3) \text{ kJ mol}^{-1}/RT] \text{ cm}^3 \text{ molecule}^{-1} \text{ s}^{-1}$					
$\text{CCl}_3 + \text{HBr} \rightarrow \text{Br} + \text{CHCl}_3$ (k_3)					
787	5.92	10.0–14.8	0.0	B_2O_3	0.06 ± 0.01

^a Temperature uncertainty: ± 1 for 299–348 K, ± 2 for 409–510 K and ± 3 for 667–787 K. ^b Errors are 1σ + Student's t and based on statistical uncertainties.

5 Hz was collimated and then directed along the axis of a heatable Pyrex reactor. The 10.5 mm id reactor was coated with halocarbon wax,[†] poly(dimethylsiloxane)[‡] or boric oxide to reduce heterogeneous reactions on the reactor wall. Gas flowing through the tube at 5 m s^{-1} was completely replaced between laser pulses. The flowing gas contained the radical precursor (typically below 0.05%), HBr in varying concentrations and the carrier gas, He, in large excess ($> 98\%$). Gas was sampled through a 0.44 mm id hole located at the end of a nozzle in the wall of the reactor and was formed into a beam by a conical skimmer before it entered the vacuum chamber containing the quadrupole mass filter. As the gas beam traversed the ion source, a portion was photoionized by VUV light and then mass selected. Temporal ion signal profiles were recorded from 10–30 ms before each laser pulse and 16–25 ms after the laser pulse with a multichannel scalar. Data from 1000 to 11 000 repetitions of the experiments were accumulated before the data were analyzed by a non-linear least-squares analysis program. At the photolysis wavelengths used to generate CH_2Br or CHBrCl radicals, it is practically impossible to photodissociate the reactant, HBr, to a measurable extent.⁶

Kinetic results from experimental studies

The chemical kinetics of the following metathetical reactions were studied separately:



Rate constants of the forward reactions (1) and (2) were combined with the rate constants of the reverse, $\text{Br} + \text{RH} \rightarrow \text{HBr} + \text{R}$,^{7,8} in order to calculate the enthalpies of formation and the experimental entropy values of the radicals. The kinetics of the reverse reactions were also calculated by *ab initio* methods. The results obtained from the experiments to measure reactions (1)–(3) are given in Table 1.

[†] Halocarbon Wax is a product of the Halocarbon Wax Corp.

[‡] Poly(dimethylsiloxane), 200 fluid was obtained from Aldrich.

Photogeneration of CH_2Br , CHBrCl and CCl_3 radicals

Up to four quartz plates were used to diminish laser fluence to a very low level. A typical radical concentration was below $10^{11} \text{ radical cm}^{-3}$. The CH_2Br radical was photogenerated by photodissociating CH_2Br_2 at 248 nm. The CH_2Br radical was formed from the precursor by C–Br bond rupture. The CHBrCl radical was photogenerated by photolysis of CHBr_2Cl at 248 nm. The CCl_3 radical was photogenerated by photolysis of CBrCl_3 at 248 nm. The primary products are $\text{CCl}_3 + \text{Br}$. A minor channel is the formation of CCl_2 .

Data analysis

Experiments were conducted under pseudo-first-order conditions where HBr existed in great excess compared with the concentration of radicals. Only the following two reactions had significant rates under these conditions:



In all sets of experiments the initial radical concentration was adjusted to be so low that radical–radical or radical–atom reactions had negligible rates compared to reactions (1)–(4). This was ensured by comparing the measured first-order wall loss decays, k_4 , of the radical with that produced (in the absence of HBr) at different conditions where precursor concentration was held steady but the laser radiation was attenuated by a factor of two using quartz plates (the radical concentration was changed by the same factor). The decays from these different experiments were equal with respect to their statistical error limits.

Rate constants for reaction (1)–(3) were obtained from the slopes of plots of the exponential radical decay constant k' vs. $[\text{HBr}]$ {from $[\text{R}^+]_t = [\text{R}^+]_0 \exp(-k't)$ }, where $k' = k_{1-3}[\text{HBr}] + k_4$. A representative ion signal decay profile and a decay constant plot from one set of experiments to measure k_1 are shown in Fig. 1. The results obtained from all the decay constant plots to measure reactions (1)–(4) are given in Table 1.

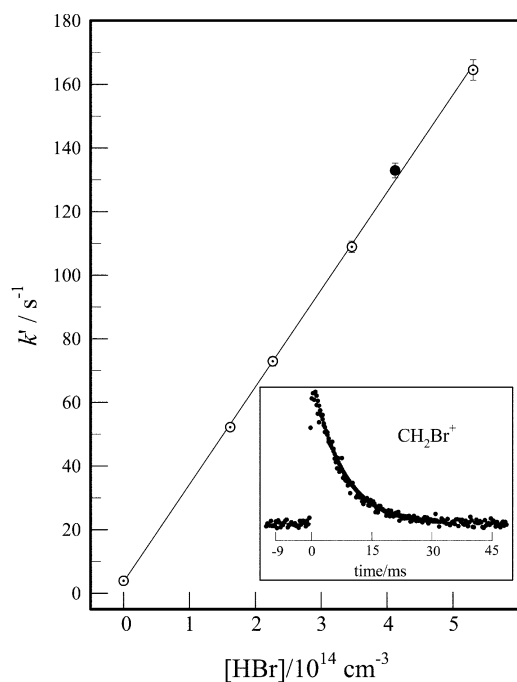


Fig. 1 Plot of first-order decay constant k' vs. $[\text{HBr}]$ for one set of experiments conducted to measure the $\text{CH}_2\text{Br} + \text{HBr}$ rate constant, k_1 , at 348 K. The inset in the lower right corner is the ion signal profile of CH_2Br^+ recorded during one of the experiments shown as a solid circle ($[\text{HBr}] = 4.12 \times 10^{13}$ molecule cm^{-3}) in the linear regression fit. The line through the data in the insert is an exponential function fitted by a nonlinear least-squares procedure. The first-order decay constant for CH_2Br^+ in the displayed ion signal profile is $(132.9 \pm 2.3) \text{ s}^{-1}$.

Accuracy of measurements

The error limits stated in Arrhenius expressions are $1\sigma + \text{Student's } t$ and they are based only on the statistical uncertainties. The reactions were studied under pseudo-first-order conditions when it was needed to know accurately only the concentration of HBr. The other errors, such as measured temperature and gas flow rates, were always $<1\%$. All these errors are very small and were thus ignored. The statistical uncertainties of the decay constants were taken into account in data analysis and their effects on the rate constants are shown in Fig. 2. The Arrhenius expression of the reaction was obtained by weighting the measured rate constants with the reciprocals of their variances for the fitting procedure.

Reagent sources and purification procedures

CH_2Br_2 , $>99\%$, CHBr_2Cl , 98% , CBrCl_3 , $>99.5\%$ and HBr, 99% , were obtained from Aldrich and helium, 99.995% , from Matheson.

The carrier gas, He, was used as provided. The radical precursors were degassed by using freeze–pump–thaw cycles and stored in darkness. HBr was collected to a flow trap kept at 77 K and was repeatedly distilled to remove any traces of bromine. HBr was stored in a dark Pyrex bulb. The flow of precursor/He mixture and HBr were not mixed until they reached the reactor. The gas handling system, which was used to set up a known HBr flow to the reactor gas inlet, was made from Pyrex glass and Teflon tubes.

Photoionization energies used

Reactants and products of the photolysis as well as the precursors were photoionized using atomic resonance radiation. A chlorine lamp (8.9–9.1 eV) coupled with a CaF_2 salt window was used to detect CH_2Br , CHBrCl or CCl_3 radicals, a

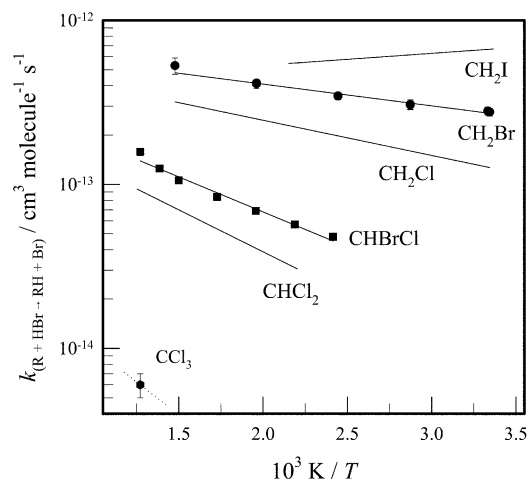


Fig. 2 Arrhenius plot of $\text{CH}_2\text{Br} + \text{HBr}$, $\text{CHBrCl} + \text{HBr}$ and $\text{CCl}_3 + \text{HBr}$ reactions measured in the current study. The dotted line shown is *ab initio* calculated threshold energy of a value of 15.3 kJ mol^{-1} . The lines are Arrhenius expressions fitted to the rate constants k_{1-3} . Three other $\text{R} + \text{HBr}$ reactions are from refs. 3 and 13.

hydrogen lamp (10.2 eV; with a MgF_2 window) to detect CCl_2 and an argon lamp (11.6, 11.8 eV; with a LiF window) to detect CH_3Br , HBr, Br_2 and Br.

Computation details

Ab initio calculations were carried out with the Gaussian 98 package of programs.⁹ All calculations were carried out on an Origin 2000 computer at the Centre for Scientific Computing (Espoo, Finland). All structures of species needed for the transition state calculations were fully optimized at the MP2 level of theory using the 6-31G(d,p) basis set and frozen-core approximation.¹⁰ The reactions of $\text{Br} + \text{CH}_3\text{Br}/\text{CH}_2\text{BrCl}$ were also calculated at the MP2(fc)/6-311G(df)//MP2(fc)/6-311G(df) level of theory for comparison (for these calculations the basis set for Br was taken from the literature).¹¹ The transition state of the equilibrium reaction was localized at the minimum energy path using a quadratic synchronous transit method (QST3).¹⁰ In the calculations the expectation values, S^2 , for free radicals were in the range of 0.7658–0.7671 and for transition states in the range of 0.7821–0.7901. Normal mode analyses were carried out at the same level of theory for all species and transition states. These frequency calculations show the optimized transition state to be a first-order saddle point with all the second derivatives of energy being positive except for one, which has an imaginary vibrational frequency along the reaction coordinate. The imaginary frequencies were in the range of -679 to -1251 cm^{-1} . The force constant matrix has only one eigenvalue. The corresponding eigenvector of the Hessian matrix is associated with the broken H–Br bond and the formed C–H bond. The relative movement of the H atom is the largest. The C–H–Br asymmetric stretch is the reaction coordinate. Furthermore, frequencies and zero-point energies of species were multiplied by a value of 0.9676 for the calculations.¹⁰ Zero-point energy corrected energies of the reactants of the reverse reactions were compared to that of the reaction transition state for the threshold energy calculation at 0 K (see Table 2). The *ab initio* calculations were used in conjunction with the thermodynamic transition state theory to determine the kinetics of the $\text{Br} + \text{molecule}$ reactions.

Computationally calculated kinetics of the reverse reactions

The results of the *ab initio* calculations at the MP2(fc)/6-31G(d,p)//MP2(fc)/6-31G(d,p) level of theory were used also

Table 2 Symmetry point groups, total and zero-point energies. Energies at the MP2(fc)/6-31G(d,p)//MP2(fc)/6-31G(d,p) level are in E_h

Compound	Symmetry	Total energy	Zero-point energy
Br	K_h	-2569.955833	0.0
HBr	$C_{\infty v}$	-2570.592802	0.006300
CH ₃ Br	C_{3v}	-2609.768741	0.038485
CH ₂ Br	C_s	-2609.101190	0.023500
CH ₂ BrCl	C_s	-3068.781685	0.029865
CHBrCl	C_1	-3068.121445	0.015953
CHCl ₃	C_{3v}	-1417.402148	0.020889
CCl ₃	C_{3v}	-1416.749188	0.007694
Br···H···CH ₂ Br	C_1	-5179.693207	0.030888
Br···Br···CH ₃	C_1	-5179.684408	0.034806
Br···H···CHBrCl	C_1	-5638.711637	0.022182
Br···Br···CH ₂ Cl	C_1	-5638.704376	0.027593
Br···Cl···CH ₂ Br	C_1	-5638.677589	0.027167
Br···H···CCl ₃	C_1	-3987.335633	0.013450

to determine entropies of the reactants and the transition states of $\text{Br} + \text{RH} \rightarrow \text{HBr} + \text{R}$ ($\text{R} = \text{CH}_2\text{Br}$ or CHBrCl) reactions (Tables 3 and 4 and ref. 12 for structural parameters, frequencies and moments of inertia). The Arrhenius expressions of the bimolecular reactions at 298.15 K were obtained using the thermodynamic transition state theory.¹³ The Arrhenius activation energies at 298.15 K were calculated from the heat capacity corrected threshold energies. The Arrhenius rate expressions of reactions (-1) and (-2) determined at 298.15 K are as follows:

$$k(\text{Br} + \text{CH}_3\text{Br} \rightarrow \text{HBr} + \text{CH}_2\text{Br}) = 4 \times 10^{-11} \exp(-64.8 \text{ kJ mol}^{-1}/RT) \text{ cm}^3 \text{ molecule}^{-1} \text{ s}^{-1}$$

$$k(\text{Br} + \text{CH}_2\text{BrCl} \rightarrow \text{HBr} + \text{CHBrCl}) = 2 \times 10^{-11} \exp(-49.7 \text{ kJ mol}^{-1}/RT) \text{ cm}^3 \text{ molecule}^{-1} \text{ s}^{-1}$$

Error limits for the A factors are not considered, for the activation energies they are typically $\pm 2.4 \text{ kJ mol}^{-1}$ in comparison of the experimentally determined activation energies with the quantum chemically calculated threshold energies.¹² The tunneling effect may increase the rate constant of reaction (-1) at 298.15 K by 45% and of reaction (-2) by 85% if Wigner correction is used. However, the tunneling effect was not used in the thermochemical calculations.

Thermochemical calculations

Both the enthalpy and entropy changes of the $\text{R} + \text{HBr} \rightleftharpoons \text{RH} + \text{Br}$ ($\text{R} = \text{CH}_2\text{Br}$ or CHBrCl) equilibria were obtained

using a second-law method. Because no mole change is involved, the standard reaction enthalpy change, $\Delta_r H^\circ$, is the difference between the activation energies of the forward and the reverse reactions. The Arrhenius expressions of the reverse reactions were either calculated from the ratios of the rate constants of $k(\text{Br} + \text{CH}_3\text{Br})/k(\text{Br} + \text{C}_2\text{H}_6)$ and $k(\text{Br} + \text{CH}_3\text{Br})/k(\text{Br} + \text{CH}_2\text{BrCl})$ and the absolute rate constant of the reaction of C_2H_6 with Br or calculated using *ab initio* methods.^{7,14} The $\Delta_r H^\circ$ was calculated from experimental studies at the middle of the overlapping temperature, T_m , ranges on a $1/T$ scale of the forward and reverse reactions.

The standard free energy change of the reaction $\Delta_r G^\circ$ and the standard entropy of the reaction $\Delta_r S^\circ$ at T_m were obtained from simple thermodynamic relations $\Delta_r G^\circ = -RT \ln K = \Delta_r H^\circ - T\Delta_r S^\circ$. The values of thermodynamic functions were corrected to 298 K using the heat capacities of reactant species. The enthalpy of formation of the radical at 298 K was calculated from the $\Delta_r H_{298}^\circ$ and the tabulated heat of formation values of the other reaction species (see Table 5). Furthermore, the entropy of the radical at 298 K was calculated from the $\Delta_r S_{298}^\circ$ and the tabulated entropy values of Br and HBr. The entropies of the CH_3Br and CH_2BrCl molecules were calculated using *ab initio* method.

The thermodynamic values obtained are as follows:

$$\Delta_f H_{298}^\circ(\text{CH}_2\text{Br}) = 171.1 \pm 2.7 \text{ kJ mol}^{-1}$$

$$S_{298}^\circ(\text{CH}_2\text{Br}) = 263 \pm 7 \text{ J K}^{-1} \text{ mol}^{-1}$$

$$\Delta_f H_{298}^\circ(\text{CHBrCl}) = 143 \pm 6 \text{ kJ mol}^{-1}$$

$$S_{298}^\circ(\text{CHBrCl}) = 294 \pm 6 \text{ J K}^{-1} \text{ mol}^{-1}$$

The C–H bond energies at 298 K were calculated directly from the enthalpies of the reactions: $E_{d,298} = -\Delta_r H_{298}^\circ(\text{R} + \text{HBr} \rightleftharpoons \text{RH} + \text{Br}) + E_{d,298}(\text{HBr})$. The C–H bond strengths obtained are $427.2 \pm 2.4 \text{ kJ mol}^{-1}$ of CH_3Br and $406.0 \pm 2.4 \text{ kJ mol}^{-1}$ of CH_2BrCl .

Discussion

Kinetics of the forward reactions

The kinetics of the CH_2Br , CHBrCl and CCl_3 radicals with HBr are shown in Fig. 2. The kinetics of the three other $\text{R} + \text{HBr}$ reactions are also given for comparison. As it is shown, halogen atom substitution at the radical site lowers the reactivity and increases the Arrhenius activation energy of the reaction. These phenomena become more obvious as the number of halogen atoms in substitution at the radical site increases. Furthermore, in series of monohalogenated methyl radicals, an I atom substituent has smallest and a Cl atom

Table 3 Structural parameters of the species optimized in *ab initio* calculations at the MP2(fc)/6-31G(d,p)//MP2(fc)/6-31G(d,p) level of theory. Bond lengths in Å and angles in degrees

Species	r_{CH}	r_{CBr}	r_{CCl}	$r_{\text{C-H}}$	$r_{\text{H-Br}}^c$	a_{BrCH}	a_{HCH}	a_{BrCCl}	a_d^d	$a_{\text{C-H-Br}}$	a_o^e
CH ₂ Br	1.075	1.865	—	—	—	116.6	122.5	—	—	—	21.3
CH ₃ Br	1.083	1.949	—	—	—	107.8	111.1	—	—	—	—
CHBrCl	1.078	1.873	1.702	—	—	115.6	—	118.9	—	—	30.2
CH ₂ BrCl	1.083	1.946	1.761	—	—	106.8	111.6	113.1	—	—	—
CCl ₃	—	—	1.713	—	—	—	—	116.8 ^a	—	—	30.2
CHCl ₃	1.083	—	1.766	—	—	—	107.5 ^b	111.3 ^a	—	—	—
Br–H–CH ₂ Br	1.081	1.869	—	1.537	1.513	114.3	118.5	—	180	173.1	36.0
Br–H–CHBrCl	1.084	1.886	1.710	1.471	1.533	112.8	—	117.5	159.4	184.6	40.0
Br–H–CCl ₃	—	—	1.727	1.411	1.559	—	—	114.7 ^a	180	180	39.0

^a Valence angle of atoms Cl–C–Cl. ^b Valence angle of atoms Cl–C–H. ^c The bond length of HBr is 1.406 Å. ^d The dihedral angle a_d is given as a_{3126} (see Fig. 3). ^e The out-of-plane angle a_o at the radical center of transition state or free radical is an angle between a plane (consists of a C and two H or two halogen atoms) and a remaining bond.

Table 4 Moments of inertia and unscaled vibrational frequencies as wavenumbers of the species calculated at the MP2(fc)/6-31G(d,p)//MP2(fc)/6-31G(d,p) level of theory. The numbers in parenthesis refer to two similar wavenumbers if given as integers

Compound	Wavenumber/cm ⁻¹	Moment of inertia/10 ⁻⁴⁷ kg m ²
CH ₂ Br	445, 711, 978, 1462, 3280, 3439	3.073, 74.85, 77.73
CH ₃ Br	631, 1003(2), 1394, 1540(2), 3174, 3303(2)	5.351, 88.40, 88.40
Br–H–CH ₂ Br	57, 315, 493, 725, 822, 888, 1010, 1187, 1460, 3230, 3371, 679i	45.95, 1096, 1136
CHBrCl	256, 548, 699, 896, 1282, 3322	19.93, 392.7, 411.9
CH ₂ BrCl	238, 629, 797, 886, 1208, 1314, 1516, 3214, 3306	28.43, 399.5, 422.6
Br–H–CHBrCl	52, 108, 250, 400, 707, 822, 874, 912, 1076, 1275, 3260, 938i	381.9, 1073, 1430
CCl ₃	289(2), 368, 526, 952(2)	249.3, 249.3, 495.3
CHCl ₃	277(2), 387, 704, 825(2), 1310(2), 3255	256.3, 256.3, 494.4
Br–H–CCl ₃	80(2), 180, 289(2), 458, 849, 881(2), 959(2), 1251i	492.2, 1119, 1119
HBr	2766	3.270

substituent has the largest effect to diminish reactivity of the radical. Clearly intramolecular electrostatic effects are present. A similar trend of decreasing radical reactivity has been demonstrated previously by R + HI reactions.¹⁸ The intramolecular electrostatic effects are explained successfully by the inductive effects of the substituents to either increase (alkyl groups) or to decrease (halogen atoms) the partial charge and the spin density at the radical site. The algebraic sum of Pauling's atomic electronegativities¹⁹ attached to the radical carbon is used as the measure of the inductive effect.¹⁸

As it is shown in Fig. 2, also a trend of the energy barriers of the R + HBr → RH + Br reactions seem to be affected by electrostatic effects. This is because $k \propto \exp(-\Delta_r G^\ddagger/RT)$. The more positive the standard free energy of activation is, the lower is the rate constant. For bimolecular reactions with no mole change $-\Delta_r G^\ddagger = T\Delta_r S^\ddagger + 2RT - E_a$. Thus the lower the rate constant, the more positive the Arrhenius activation energy because the entropy factor is always negative. The $\Delta_r S^\ddagger$ is typically $-120 \text{ J K}^{-1} \text{ mol}^{-1}$. The standard free energy of activation is related to electrostatic effects of the radical. This is shown in Fig. 4 by plotting $\Delta_r G^\ddagger$ values at 298.15 K vs. Δ electronegativity values of the radicals. The plot is linear. The more positive $\Delta_r G^\ddagger$ value, the slower is the reaction. This is in perfect agreement with Fig. 2.

Complex reaction system

Generally metathetical R + HBr reactions are considered to occur *via* two transition states. The radical may initially be attracted loosely to the Br end of HBr to form an adduct complex. This seems to be reasonable because Br is more electronegative than H, and has stronger tendency and larger size to form a bond with the radical carbon. This bond formation should become more obvious with bulky alkyl radicals because large electronegativity difference between the radical carbon and the Br end of HBr compared to the H end of HBr should favour a strong bond formation. However, this channel is strongly endothermic and thus may finally not proceed any further. The HBr molecule has to rotate before the exothermic

Table 5 Heats of formation and entropies used in the thermochemical calculations

Species	$\Delta_f H^\circ_{298}/\text{kJ mol}^{-1}$	$S^\circ_{298}/\text{J K}^{-1} \text{ mol}^{-1}$
HBr ^d	-36.44 ± 0.17	198.70
Br ^d	111.86 ± 0.06	175.02
CH ₃ Br ^{b,c}	-38.1 ± 1.3	245.29
CH ₂ BrCl ^{d,c}	-45.0 ± 5.0	286.49

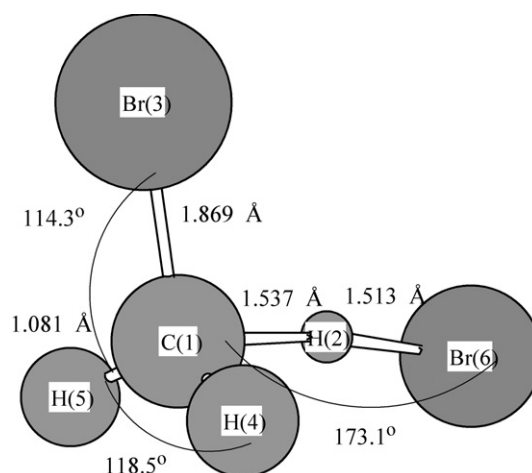
^a Data taken from ref. 15. ^b Data taken from ref. 16. ^c This work.

^d Data taken from ref. 17.

reaction channel can take over. During the rotation period also a bent adduct complex could be formed but threshold energy of such reaction is even higher than to form a linear adduct complex.¹² After the rotation, the R···H–Br van der Waals complex proceeds to a transition state, which structure is tighter than that of the adduct complex. The transition state is affected by electrostatic effects. These effects seem to affect the structure and the density of energy levels more for an alkylated transition state than for a halogenated transition state.¹² With high density of energy levels, the transition state can more easily be thermally activated as temperature of the reaction increases. Moreover, a thermally excited transition state should have a feature to fall apart to reactants more easily and the overall rate constant should decrease with increasing temperature. This has been observed with radical + HBr reactions in time-resolved experimental studies by various mass spectrometric and spectroscopic techniques.^{20,21}

Kinetics of the reverse reactions

The *ab initio* calculated Arrhenius rate expressions for the Br + CH₃Br and Br + CH₂BrCl reactions are relative accurate compared to the experimental values available.^{7,8,14} The difference between the Arrhenius activation energies is only 0.4 kJ mol⁻¹ for the reaction (–1) and 0.7 kJ mol⁻¹ for the reaction (–2). The largest disagreement can be found between the *A* factors. For reaction (–1) the *ab initio* calculated *A* factor is by a factor of four smaller than that of the experimental value. For reaction (–2) a similar factor is 1.6, respectively. The tunneling is not considered here. However, if one takes into

**Fig. 3** Optimized transition state of the Br + CH₃Br → CH₂Br + HBr reaction at 0 K. The parameters are calculated at the MP2(fc)/6-31G(d,p)//MP2(fc)/6-31G(d,p) level of theory. The dihedral angle $a_d = a_{3126} = 180^\circ$.

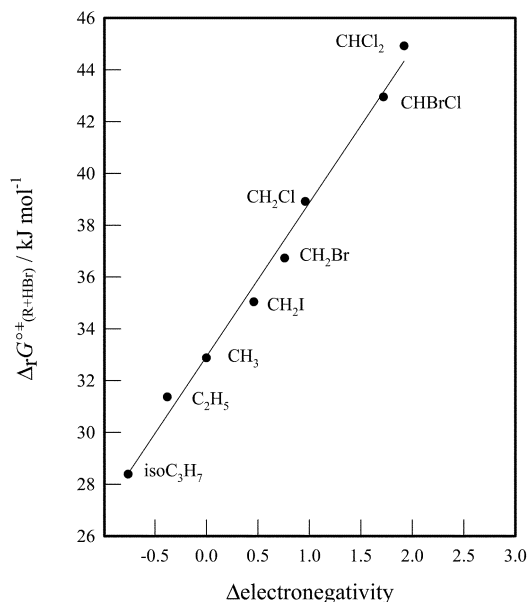


Fig. 4 Plot of the standard free-energy of activation at 298.15 K of some R + HBr reactions vs. Δelectronegativity of R.

account the error limits of the experimental A factors given, which are from 55 to 60%, the disagreement is relative small.

The product of reaction (1) was detected to be CH₃Br. The transition states of the two reaction channels of Br + CH₃Br reaction and the three reaction channels of Br + CHBrCl reaction were characterized (see Table 2 for energies). In general, the energy barrier for abstracting an H atom by the Br atom on CH₃Br is about 33 kJ mol⁻¹ smaller than the competing channel for abstracting a Br atom. On the other hand, the Br atom can abstract an H atom, a Br atom or a Cl atom on CH₂BrCl. For these the energy barriers at 0 K are 48.4, 81.2 and 150.5 kJ mol⁻¹. Clearly the Br + CH₂BrCl → HBr + CHBrCl channel dominates.

The threshold energies of reactions (-1 and -2) at 0 K were also calculated at the MP2(fc)/6-311G(df)//MP2(fc)/6-311G(df) level of theory for comparisons. The zero-point energy corrected threshold energy of reaction (-1) is 62.3 kJ mol⁻¹ and of reaction (-2) is 50.3 kJ mol⁻¹ (zero-point energies were scaled by a factor of 0.95). On the other hand the previously used MP4/6-311++G(3d,2p)//MP2(fc)/6-31G(d,p) level of theory does not apply here.²² This level of theory used for the QST3 calculations yielded a value of 51.0 kJ mol⁻¹ for abstraction an H atom on bromomethane by the Br atom at 0 K (reaction (-1)). This is clearly too low value and implies that this level of theory is not suitable for threshold energy calculations of the reactions studied.

Enthalpy of formation values determined

The enthalpy of formation of the CH₂Br radical was found to be 171.1 ± 2.7 kJ mol⁻¹ at 298 K. This value is in very good agreement with the value of 170.3 ± 8.4 kJ mol⁻¹ from the appearance energy measurement of Holmes and Lossing.²³ The other determination by them gave 168.2 ± 8.4 kJ mol⁻¹.²⁴ Tschuikow-Roux and Paddison determined the heat of formation of the CH₂Br radical to be 169.0 ± 4.1 kJ mol⁻¹.²⁵ The value is based on the analysis of thermochemical and kinetic data on the bromination of bromomethane.

The Δ_fH₂₉₈[°] (CHBrCl) was found to be 143 ± 6 kJ mol⁻¹. This seems to be the first experimental enthalpy of formation determination for the CHBrCl radical. Espinosa-García and Dóbbé used hydrogenation and isodesmic reactions with an *ab initio* method at the MP4(SDTQ)(fc)/6-311++G(3d,2p)//

MP2(full)/6-31G(d,p) level of theory (also Gaussian G2 theory) to calculate Δ_fH₂₉₈[°] (CHBrCl) to be 147 ± 6 kJ mol⁻¹.²⁶

The C–H bond strength of halogenated methanes

The C–H bond strength of CH₃Br is 427.2 ± 2.4 kJ mol⁻¹ and of CH₂BrCl is 406.0 ± 2.4 kJ mol⁻¹. These values are in very good accord with the values of the other halogenated methanes. The C–H bond strength decreases from methane to chloroform in the following order (values in kJ mol⁻¹ and determined experimentally): methane (437.9)³ > iodomethane (431.6)¹³ > bromomethane (427.2) > chloromethane (419.0)³ > bromochloromethane (406.0) > dichloromethane (402.5)³ > chloroform (393.9)³. Experimentally determined Arrhenius activation energies of an H atom abstraction reaction by the Br atom on a substituted methane are as follows (in kJ mol⁻¹): methane (76.1) > iodomethane (63.9)¹³ ≈ bromomethane (64.4) > chloromethane (57.7) > bromochloromethane (49.0) > dichloromethane (47.0) > chloroform (38.9).¹² Clearly, the energy barrier of Br + substituted methane reaction becomes smaller parallel to the trend of decreasing C–H bond strength from methane to chloroform. These trends are most likely caused by intramolecular electrostatic effects where electronegative halogen atoms make the C–H bond weak in a similar manner as they affect to the reactivity of halogenated methyl radicals.

Frequencies for CH₂Br. The ground state electronic configuration of the pyramidal CH₂Br radical could be: ... (5a'')²(14a')²(15a'')²(6a'')²(16a')² ²A' (C_s). The calculated vibrational frequencies given as wavenumbers of the CH₂Br are shown in Table 4. As expected, the radical has six normal modes, which span the representation Γ = 4a' + 2a''. The values are compared to the experimental values, which are measured in an argon matrix.²⁷ Of these 368 cm⁻¹ umbrella mode is very strong, 693 cm⁻¹ CBr stretch and 1356 cm⁻¹ CH₂ scissors are strong modes, and 953 cm⁻¹ CH₂ rock mode is weak. The equivalent *ab initio* calculated scaled values (by 0.9676) for an anharmonic correction are 430, 688, 1414, 947 cm⁻¹ (two other 3174 cm⁻¹ CH₂ symmetric stretch and 3328 cm⁻¹ CH₂ asymmetric stretch are weak). All wavenumbers calculated except the umbrella mode have similar values and similar relative intensities as the experimental ones. This was expected. The *ab initio* program calculates a harmonic frequency which does not apply to the umbrella mode. Because the CH₂Br radical is pyramidal, the umbrella (or OPLA) mode of the radical is not harmonic. This mode should possess two potential energy minima along the umbrella coordinate. As the barrier of inversion becomes smaller, the increased interaction of the two wave functions on the potential energy minima causes the degeneracy of the energy levels to be split. The degree of splitting is largest at higher vibrational levels near the top of the inversion barrier, where the energy levels can not be taken to be harmonic. A similar phenomenon has been calculated for the CHCl₂ radical.²⁸

Thermochemical functions of the CH₂Br. Ideal gas thermodynamic parameters C_p[°], S[°], -(G[°] - H₀[°])/T and (H[°] - H₀[°]) were calculated by the statistical thermodynamic method based on a rigid rotor harmonic oscillator model. The values were tabulated in a JANAF manner. For this also Δ_fH[°], Δ_fG[°] and log₁₀K_f were calculated as a function of temperature. The heat of formation values were fitted to give a kinetically determined value at 298.15 K. For the calculations (H[°] - H₀[°]) and S[°] values for elements were taken from the literature. For these calculations the *ab initio* calculated umbrella mode wavenumber was replaced by the more reliable experimental value of 368 cm⁻¹. This is because low frequency modes have the strongest effect to the calculated thermodynamic parameters. All the other calculated wavenumbers were multiplied by 0.9676 for

Table 6 Ideal gas thermochemical functions for the CH₂Br radical at a standard state of 1 bar

T/K	C _p ^o /J K ⁻¹ mol ⁻¹	S ^o /J K ⁻¹ mol ⁻¹	[-(G ^o - H ^o)/T]/J K ⁻¹ mol ⁻¹	H ^o - H ₀ ^o /kJ mol ⁻¹	Δ _f H ^o /kJ mol ⁻¹	Δ _f G ^o /kJ mol ⁻¹	log ₁₀ K _f
100	34.482	217.953	184.469	3.348	180.5	171.6	-89.61
200	39.961	243.453	208.158	7.059	178.8	163.3	-42.65
298.15	45.518	260.465	222.702	11.259	171.1 ^a	156.8	-27.47
300	45.616	260.747	222.936	11.343	171.0	156.7	-27.28
400	50.357	274.544	234.168	16.151	154.7	155.2	-20.27
500	54.093	286.199	243.438	21.381	153.8	155.5	-16.24
600	57.084	296.335	251.427	26.945	153.0	155.9	-13.57
700	59.599	305.328	258.497	32.782	152.3	156.4	-11.67
800	61.809	313.434	264.866	38.854	151.6	157.1	-10.26
900	63.796	320.830	270.679	45.136	151.0	157.8	-9.16
1000	65.596	327.647	276.039	51.607	150.4	158.6	-8.28
1100	67.226	333.977	281.022	58.250	149.9	159.4	-7.57
1200	68.696	339.890	285.684	65.047	149.5	160.3	-6.98
1300	70.016	345.442	290.069	71.984	149.1	161.2	-6.48
1400	71.197	350.674	294.213	79.046	148.8	162.2	-6.05
1500	72.251	355.623	298.144	86.219	148.5	163.2	-5.68

^a Current study.

the anharmonic correction as has been suggested in the literature.¹⁰ The standard state for the calculated values is 1 bar. The JANAF tabulated parameters for a temperature range of 100–1500 K are shown in Table 6.

Summary

The kinetics of CH₂Br, CHBrCl and CCl₃ radical reaction with HBr have been characterized. The temperature dependence measured was combined with the temperature dependence of the reverse reaction to obtain the enthalpy of formation of CH₂Br radical to be 171.1 ± 2.7 kJ mol⁻¹ and of CHBrCl radical to be 143 ± 6 at 298 K. The different reaction channels of reverse reactions were studied by the *ab initio* methods. The C–H bond strength of bromomethane was calculated to be 427.2 ± 2.4 kJ mol⁻¹ and of bromochloromethane was calculated to be 406.0 ± 2.4 kJ mol⁻¹. The thermochemical functions for the CH₂Br radical are calculated and given in a JANAF manner.

Acknowledgements

This research was supported by the University of Helsinki, the Center for Scientific Computing at Espoo (both in Finland) and the National Science Foundation, Chemistry Division (USA). I thank Dr Dóbe for showing me the preliminary kinetic results of his and K. Imrik's investigations concerning the reaction of CH₂BrCl with Br atom. I also wish to thank Prof. Irene R. Slagle for kindly lending me the experimental apparatus for this study. The kinetic experiments were carried out at the Catholic University of America (Washington DC, USA).

References

- 1 A. Jordan, J. Harnisch, R. Borchers, F. le Guern and H. Shinohara, *Environ. Sci. Technol.*, 2000, **34**, 1122.
- 2 K. Pfeilsticker, W. T. Sturges, H. Bösch, C. Camy-Peyret, M. P. Chipperfield, A. Engel, R. Fitzenberger, M. Müller, S. Payan and B.-M. Sinnhuber, *Geophys. Res. Lett.*, 2000, **27**, 3305.
- 3 J. A. Seetula, *J. Chem. Soc., Faraday Trans.*, 1996, **92**, 3069.
- 4 I. R. Slagle and D. Gutman, *J. Am. Chem. Soc.*, 1985, **107**, 5342.
- 5 J. A. Seetula, *Ann. Acad. Sci. Fenn. Ser. A2*, 1991, 234.
- 6 B. J. Huebert and R. M. Martin, *J. Phys. Chem.*, 1968, **72**, 3046.

- 7 G. C. Fettes and J. H. Knox, in *Progress in Reaction Kinetics*, ed. G. Porter, Pergamon, New York, 1964, vol 2, p. 1.
- 8 A private discussion with Dr S. Dóbe.
- 9 M. J. Frisch, G. W. Trucks, H. B. Schlegel, G. E. Scuseria, M. A. Robb, J. R. Cheeseman, V. G. Zakrzewski, J. A. Montgomery, Jr., R. E. Stratmann, J. C. Burant, S. Dapprich, J. M. Millam, A. D. Daniels, K. N. Kudin, M. C. Strain, O. Farkas, J. Tomasi, V. Barone, M. Cossi, R. Cammi, B. Mennucci, C. Pomelli, C. Adamo, S. Clifford, J. Ochterski, G. A. Petersson, P. Y. Ayala, Q. Cui, K. Morokuma, D. K. Malick, A. D. Rabuck, K. Raghavachari, J. B. Foresman, J. Cioslowski, J. V. Ortiz, B. B. Stefanov, G. Liu, A. Liashenko, P. Piskorz, I. Komaromi, R. Gomperts, R. L. Martin, D. J. Fox, T. Keith, M. A. Al-Laham, C. Y. Peng, A. Nanayakkara, M. Challacombe, P. M. W. Gill, B. Johnson, W. Chen, M. W. Wong, J. L. Andres, C. Gonzalez, M. Head-Gordon, E. S. Replogle and J. A. Pople, *Gaussian 98, Revision A.3*, Gaussian Inc., Pittsburgh PA, 1998.
- 10 J. B. Foresman and Æ. Frisch, *Exploring Chemistry with Electronic Structure Methods*, Gaussian Inc., Pittsburgh, 2nd edn., 1996.
- 11 M. N. Glukhovtsev, A. Pross, M. P. McGrath and L. Radom, *J. Chem. Phys.*, 1995, **103**, 1878.
- 12 J. A. Seetula, *Phys. Chem. Chem. Phys.*, 2000, **2**, 3807.
- 13 J. A. Seetula, *Phys. Chem. Chem. Phys.*, 2002, **4**, 415.
- 14 P. W. Seakins, M. J. Pilling, J. T. Niiranen, D. Gutman and L. N. Krasnoperov, *J. Phys. Chem.*, 1992, **96**, 9847.
- 15 M. W. Chase, Jr., C. A. Davies, J. R. Downey, Jr., D. J. Frurip, R. A. McDonald and A. N. Syverud, *J. Phys. Chem. Ref. Data*, 1985, **14**, Suppl. No.1.
- 16 J. Bickerton, M. E. M. da Piedade and G. Pilcher, *J. Chem. Thermodyn.*, 1984, **16**, 661.
- 17 L. V. Gurvich, V. S. Iorish, D. V. Chekhovskoi and V. S. Yungman, *IVTANTHERMO, NIST Database 5*, National Institute of Standards and Technology, Gaithersburg, MD, 1993.
- 18 J. A. Seetula and D. Gutman, *J. Phys. Chem.*, 1991, **95**, 3626.
- 19 L. Pauling, *Nature of the Chemical Bond*, Cornell University Press, Ithaca, NY, 3rd edn., 1960.
- 20 J. A. Seetula and I. R. Slagle, *J. Chem. Soc., Faraday Trans.*, 1997, **93**, 1709.
- 21 P. D. Richards, R. J. Ryther and E. Weitz, *J. Phys. Chem.*, 1990, **94**, 3663.
- 22 J. Espinosa-García, *Mol. Phys.*, 1999, **97**, 629.
- 23 J. L. Holmes and F. P. Lossing, *Int. J. Mass Spectrom. Ion Proc.*, 1984, **58**, 113.
- 24 J. L. Holmes and F. P. Lossing, *J. Am. Chem. Soc.*, 1988, **110**, 7343.
- 25 E. Tschuikow-Roux and S. Paddison, *Int. J. Chem. Kinet.*, 1987, **19**, 15.
- 26 J. Espinosa-García and S. Dóbe, *J. Phys. Chem. A*, 1999, **103**, 6387.
- 27 *NIST Webbook*, National Institute of Standards and Technology, Gaithersburg, MD, <http://webbook.nist.gov/>.
- 28 S. A. Kafafi and J. W. Hudgens, *J. Phys. Chem.*, 1989, **93**, 3474.